Identifying Global Anatomical Differences: Deformation-Based Morphometry

John Ashburner, Chloe Hutton, Richard Frackowiak, Ingrid Johnsrude, Cathy Price and Karl Friston

The Wellcome Department of Cognitive Neurology, Institute of Neurology, Queen Square, London WC1N 3BG, United Kingdom

Running Title Anatomical Differences

Keywords morphometrics, anatomy, spatial normalization, multivariate analysis.

Address for correspondence

Wellcome Department of Cognitive Neurology,
Functional Imaging Laboratory,
12 Queen Square,
London. WC1N 3BG
U.K.

Tel +44 (0)171 833 7472

Fax +44 (0)171 813 1420

email j.ashburner@fil.ion.ucl.ac.uk

Abstract

The aim of this paper is to illustrate a method for identifying macroscopic anatomical differences among the brains of different populations of subjects. The method involves spatially normalizing the structural MR images of a number of subjects so that they all conform to the same stereotactic space. Multivariate statistics are then applied to the parameters describing the estimated nonlinear deformations that ensue. To illustrate the method, we have compared the gross morphometry of male and female subjects. We also assessed brain asymmetry, the effect of handedness, and the interactions among these effects.

1 Introduction

In this paper we introduce a new technique to characterize differences among structural or anatomical brain images. The anatomical differences between any two brains can be expressed at a microscopic scale (e.g. differences in cytoarchitectonics or myeloarchitectonics), at a mesoscopic scale (e.g. cortical dysplasia) or at a macroscopic level (e.g. ventricular enlargement or abnormal temporal lobe asymmetry). From the perspective of neuroimaging, differences at a mesoscopic and macroscopic level are amenable to measurement. We have recently developed a technique that looks for differences at a mesoscopic scale (i.e. several millimeters) called *voxel-based morphometry* and have demonstrated it in relation to regionally specific abnormalities in grey matter in schizophrenia (Wright *et al.*, 1995). This approach uses spatially normalized, segmented images in conjunction with statistical parametric mapping to provide inferences about differences in the local density of various tissue compartments (e.g. gray matter or white matter). Voxel-based morphometry throws away macroscopic or global differences in anatomy at the spatial normalization step. Here we describe a technique that characterizes these global differences in macroscopic anatomy that complements voxel-based morphometry, allowing one to examine differences at both mesoscopic and macroscopic scales.

By analogy with voxel-based morphometry we have called this new approach *deformation-based morphometry*. Both can be seen as developments in the growing field of computational neuroanatomy. Deformation-based morphometry is a characterization of the differences in the vector fields that describe global or gross differences in brain shape. These vector fields are the deformation fields used to effect nonlinear variants of spatial normalization, when one of the images is a template that conforms to some standard anatomical space. In what follows we take the deformation fields that map a series of images onto the same template, and then compare them to see if there are any systematic differences. Because the deformation fields are multivariate, we employ standard multivariate statistical techniques to estimate the nature of the differences and to make inferences about them. The endpoint of deformation-based morphometry is a p value pertaining to the significance of the effect and one or more canonical vectors, or deformations, that characterize their nature. These results are obtained

using multivariate analysis of covariance (ManCova) and canonical variates analysis (CVA) respectively.

The importance of this technique is that it is completely automated and therefore completely reliable. Its validity is established in terms of the estimation of the deformation fields and the templates used in the analysis. Thirdly, there is no implicit bias in terms of which anatomical differences might be identified.

Studies of brain morphometry have been carried out by many researchers on a number of different populations, including patients with schizophrenia, autism, dyslexia and Turner's Syndrome. In relation to schizophrenia, much of the work has focussed on the dimensions of the temporal lobes (Crow, 1990; Bartzokis *et al.*, 1996; Jacobsen *et al.*, 1996), hippocampal volumes (Suddath *et al.*, 1990; Altshuler *et al.*, 1990), ventricle volumes (Suddath *et al.*, 1990; Blackwood *et al.*, 1991; Lieberman *et al.*, 1992), anterior cingulate and frontal lobes (Noga *et al.*, 1995; Nopoulos *et al.*, 1995), basal ganglia (Frazier *et al.*, 1996) and also whole brain volumes. Other areas of research include sexual dimorphism of schizophrenic brains (Nasrallah *et al.*, 1990) and the degree of asymmetry (Crow, 1990). Abnormal cerebellar morphology has been found in autism (Ciesielski & Knight, 1994), along with differences in the morphology of the forebrain - especially the anterior ventricular horns, lateral ventricles and right ventricular nucleus (Gaffney *et al.*, 1989). Autistic brains have also been found to be more symmetric than control brains (Tsai *et al.*, 1983). Differences found in Turner's syndrome include smaller volumes of a number of brain structures (Murphy *et al.*, 1993), and different regional distributions of gray and white matter in both right and left parietal regions (Reiss *et al.*, 1995).

Often, the morphometric measurements used in these studies have been obtained from brain regions that can be clearly defined, resulting in a wealth of findings pertaining to these particular measurements. These measures are typically volumes of unambiguous structures such as the hippocampi or the ventricles. However, there are a number of morphometric features that may be rather more difficult to quantify by inspection, meaning that many structural differences may be overlooked. In summary the study of macroscopic anatomical dimorphism is an important field that has provided a number of intriguing insights into the pathogenesis or neuro-developmental aspects of several neuropsychiatric disorders. It is the case however that most studies to date have focussed on anatomical 'metrics' that are easy to measure. These may, or may not be, germane to the pathophysiology under investigation. The importance of the approach described here is that it is not biased in any way to one particular structure or tissue and gives an even-handed and comprehensive assessment of anatomical differences throughout the brain.

In Friston *et al.* (1995b) we observed that: "The topography of an image can be characterized in terms of the coefficients corresponding to the spatial basis functions. This simple list of coefficients, taken in conjunction with the reference image, is a complete specification of the original image (down to the resolution imposed by the basis functions). The importance of this observation is that anatomical topography can be characterized by a multivariate measure (the coefficients) and subject to conventional mulitvariate statistics". What follows

is an implementation of that basic idea.

In order to demonstrate the technique we have chosen to study dimorphism in relation to handedness and sex. This should be seen as a vehicle to explain and illustrate how to do these analyses. The paper is divided into a methods section, that describes the approach and a short results section. The details of the statistical analysis are presented in an appendix for the interested reader and represent standard methods that have already been applied to functional imaging data (Friston *et al.*, 1995a).

2 Method

High resolution structural T1 MR images were acquired from 61 normal healthy volunteers. These were all acquired on the same 2 Tesla Siemens Magnetom Vision scanner, using an MPRAGE sequence. The resolution of the images was $1mm \times 1mm \times 1.5mm$. The data consisted of 15 female right-handed subjects, 5 female left-handed subjects, 30 male right-handed subjects and 11 male left-handed subjects, all between the ages of 20 and 37. The scans were all acquired as part of ongoing functional imaging projects within the department, and all subjects had no neurological or psychiatric history.

The images were spatially normalized by a least squares match to a template image. This template consisted of an average of twelve 12-parameter affine registered T1 MR images of the head, and was rendered symmetric by averaging with itself reflected across the saggital midplane. The MRI sequence used to generate the images, constituting the template, was identical to that used for all the other images, thus ensuring that more accurate registrations could be achieved.

The first step of the normalization was to determine the optimum 12-parameter affine transformation (Ashburner *et al.*, 1997). Initially, the registration was performed by matching the whole of the head (including the scalp) to the template. Following this, the registration proceeded by only matching the brains together, by appropriate weighting of the template voxels (see figure 1). This is a completely automated procedure (that does not require "scalp editing") that discounts the confounding effects of skull and scalp differences.

[Figure 1 about here.]

The affine registration was followed by estimating nonlinear deformations, whereby the deformations are defined by a linear combination of three dimensional discrete cosine transform (DCT) basis functions (Ashburner & Friston, 1998; Friston *et al.*, 1995b). Each of the deformation fields was described by 1176 parameters, where these represent the coefficients of the deformations in three orthogonal directions. The matching involved simultaneously minimizing the membrane energies of the deformation fields and the residual squared difference between the images and template as described previously. The mean of the spatially

normalized images is shown for each group in figure 2. It can be seen that in terms of gross anatomy, following normalization, they are virtually indistinguishable.

[Figure 2 about here.]

Each set of spatial normalization parameters (affine and nonlinear) encodes a deformation field relating to the position, size and shape of the brain. For the analysis presented here, we used only the information relating to the shapes of the brains, by removing the effects of size and position (see Appendix B).

Following this, a matrix $\mathbf{A_0}$ was generated, where each row contained the coefficients of the nonlinear basis functions describing the difference in shape between the template and each image. For the multivariate analysis that followed, it was necessary to reduce the number of these coefficients relative to the number of images. Principal component analysis was used to compact this information, such that about 96% of the variance of the nonlinear deformations was represented by 20 parameters for each image. This dimension reduction used singular value decomposition to decompose matrix $\mathbf{A_0}$ into unitary matrixes $\mathbf{U_0}$ and $\mathbf{V_0}$, and diagonal matrix $\mathbf{S_0}$, such that $\mathbf{A_0} = \mathbf{U_0 S_0 V_0}^T$. Matrix $\mathbf{S_0}$ was reduced to a smaller diagonal matrix $\mathbf{S}$, by eliminating the rows and columns containing the least important components. The same columns were removed from $\mathbf{U_0}$ to produce the matrix $\mathbf{U}$. The reduced data ($\mathbf{A}$ of dimension $m \times n$) was constructed with $\mathbf{A} = \mathbf{US}$.

Multivariate analysis of covariance (ManCova) was used to make inferences about the effects of interest (i.e. provide p values). In the simplest case of comparing two groups, the ManCova becomes the special case of Hotelling's T^2 test. ManCova does not simply tell one what the difference is. To characterize these differences one usually uses canonical variates analysis (CVA) based upon the parameters estimates from the ManCova. CVA is a device that finds the linear combination of the dependent variables (in this case the deformations) that is maximally correlated with the explanatory variables (e.g. male vs. female). In the simple case of one categorical explanatory variable (e.g. sex) this will be the deformation field that best discriminates between males and females. Note that this is not the same as simply subtracting the deformation fields of two groups. This is because (i) the ManCova includes the effects of confounds that are removed and (ii) some aspects of the dimorphic deformations may be less reliable than others (CVA gives deformations that explicitly discount error in relation to predicted differences). The canonical deformations can either be displayed directly as deformation fields, or can be applied to some image to "caricature" the effect detected. In this paper, we combine both in order to illustrate the deformations more clearly.

3 Results

Tests for significant differences between groups of subjects were performed using a ManCova (see Appendix A) on the deformation parameters. A number of tests were performed, in-

cluding tests relating to the handedness of the subjects, of sexual dimorphism, looking at brain asymmetry, and interactions among these factors. A full report of these results will be presented elsewhere. Here we concentrate on a few of the more illuminating analyses.

3.1 Handedness, Sex and the Interaction Between Them

A ManCova testing for the effects of both handedness and sex simultaneously, suggested extremely significant effects ($p = 2.1 \times 10^{-7}$). Because there were two effects of interest, CVA (see Appendix A) could be used to generate a scatter-plot representing the optimum separation of the groups (see figure 3) in terms of the two corresponding canonical variates. It can be seen that the first canonical variate is mainly sensitive to the differences between men and women, whereas the second discriminates between handedness.

[Figure 3 about here.]

The effects of sex and handedness were then tested individually, both showing significant differences ($p = 0.00014$ and $p = 0.00020$ respectively). The test for sex differences used handedness as a confound and that for handedness used sex as a confound. A further test failed to show any interaction between handedness and sex ($p = 0.90$). The differences between the groups were characterized using CVA; The results are illustrated in figure 4. These can be compared to the difference between the brain shapes (after removing confounding effects) as shown in figure 5. We will comment on the differences between the two sorts of characterization (CVA and those based directly on the parameter estimates) below.

The effect of sex can be most clearly seen in the saggital view and suggests that men have a more protruding occipital pole, whereas women have more prominent frontal poles. The effect of handedness involves more asymmetric differences affecting predominantly the right frontal lobe (transverse section, middle row of figure 4).

[Figure 4 about here.]

[Figure 5 about here.]

3.2 Brain Asymmetry

Because the template used by the spatial normalization was symmetrical, it was possible to look at left/right brain asymmetry. The coefficients of the DCT can be divided into those that account for non-linear deformations that are symmetric, and those that relate to anti-symmetric deformations. Very significant brain asymmetries were detected ($p = 0.0$) by testing that the coefficients of the anti-symmetric warps differed from zero. Geschwind

& Galaburda (1987) discuss many of the asymmetries found by a number of researchers. These include the fact that the left occipital lobe is broader and longer than that on the right, which is confirmed in figure 5. However, because of the large amount of variability in the occipital lobes, this is not a feature of brain asymmetry that is strongly characterized by CVA (see figure 4). Another asymmetry (that was not really confirmed in Geschwind & Galaburda) is that the right frontal lobe is usually larger than that on the left. However, the results we obtain contradict this finding, in that the left frontal lobe appears to be the larger of the two. From figure 5 we see that the magnitude of the difference is relatively small, but it is still a feature that is strongly characterized by CVA. Differences in asymmetry between males and females and between left and right handed subjects were both found to be significant ($p = 0.026$ and $p = 0.0076$ respectively), and will be presented elsewhere.

In short, reliable features of asymmetry and dimorphism may not necessarily be the biggest or most obvious. Furthermore, the approach presented here gives estimates of dimorphism that explicitly discount differences due to other factors, in this instance sex and handedness.

4 Discussion

In this paper we have introduced deformation-based morphometry. This technique allows one to characterize and make inferences about the differences in macroscopic anatomy among structural brain images and can be seen as the complement to voxel-based morphometry. The latter deals with residual, local differences in tissue compartment composition once the macroscopic differences have been removed. In brief the parameters describing the mapping of the images to some common template are reduced using SVD and then subject to ManCova to provide parameter estimates and statistical inferences. CVA can then be employed to give deformations that best capture the effect one is interested in.

We anticipate that the power of the approach will be realized when several explanatory variables are considered together in multifactorial designs. In this case there will be a series of canonical deformations and compounds of explanatory variables that fully characterize the nature of the differences. An intriguing example of this approach would be to examine the effect of being schizophrenic, age and the interaction between these factors. This interaction may point to a putative degenerative process in schizophrenia that eschews the necessity to acquire longitudinal data (which is very difficult to do). An interaction here would imply that schizophrenic anatomy changes with time at a different rate to that predicted by normal age-related changes.

One important aspect of deformation-based morphometry is that the entire brain is examined in a balanced way. This may be important in the sense that correlated changes in morphology between anatomically connected but distant brain regions will be evident in a way that would be missed by just looking at one, easily identified, structure. In terms of characterizing the effects we have used CVA and the parameter estimates directly (i.e., differences having adjusted for confounds). The latter approach is a special case, due to

having just one effect of interest, of using the eigenvectors of the fitted effects. This is an alternative to CVA which uses the generalized eigenvectors of the fitted effects and error. Both are useful characterizations and can be used to complement each other: The simple eigenvectors show which warps are the biggest, whereas the canonical vectors give effects that are more reliable.

The current paper has some features in common with the work of Bookstein (1997). Both papers use multivariate statistics to differentiate between the brain shapes of different populations. The measure of shape used by the two papers is also similar. However, the methods differ principally in that the current approach utilizes the more general statistical method of ManCova, rather than the special case of Hotelling's T^2 test. In addition, the estimates of shape are based upon the whole brain, rather than a two dimensional section through the corpus callosum, and are identified automatically rather than relying upon manual landmark identification.

There are many features of deformation fields that could be used to characterize differences in brain shape, and so could be included in such tests. In principle, the Jacobians of the transformations (a matrix field relating to the spatial derivatives of the transformation) should be more reliable indicators of brain shape than absolute deformations (since absolute deformations need to be quantified relative to some arbitrary reference position). One simple feature of a Jacobian that could be considered is the determinant, which directly encodes the relative volume of the brain region. With more sophisticated Bayesian image registration methods, more control is exerted over the nature of the distributions from which the parameters are drawn. The parameter estimates may no longer be normally distributed, so simple tests based upon assumptions of normality would not be appropriate. It is envisaged that future work on morphometry should develop in concurrence with the methods used for estimating the deformations. The parameter distributions imposed upon the deformations by the registration method could be used in the morphometry studies. Similarly, knowledge of the variability of brain shapes obtained from morphometry could be used as *a priori* information for Bayesian image registration methods. Both fields would clearly benefit by having a compact and concise representation of the anatomical variability of brains.

Cao and Worsley (1997; 1997) have also described a multivariate approach to morphometry. This approach belongs to the voxel-based morphometry class in that the multivariate inferences are about regionally specific differences (therein producing an SPM) and addresses things like displacement of the cortical surface from some normal position. In this instance the multivariate nature of the analyses pertains to the vectorial displacements at each voxel, not to the vector-fields that subsume all voxels. Approaches such as this and the one described in this paper speak to an exciting and progressive refinement of computational neuroanatomy in imaging neuroscience.

Acknowledgements

Thanks to all the fellows at the Wellcome Department of Cognitive Neurology who (knowingly or otherwise) provided data for this project. This work was supported by the Wellcome Trust.

References

Altshuler, L. L., Casanova, M. F., Goldberg, T. E., & Kleinman, J. E. 1990. The Hippocampus and Parahippocampus in Schizophrenia, Suicide, and Control Brains. *Arch. Gen. Psychiatry*, **47(11)**, 1029–1034.

Ashburner, J., & Friston, K. J. 1998. Nonlinear Spatial Normalization using Basis Functions. *submitted to Human Brain Mapping.*

Ashburner, J., Neelin, P., Collins, D. L., Evans, A. C., & Friston, K. J. 1997. Incorporating Prior Knowledge into Image Registration. *NeuroImage*, **6**, 344–352.

Bartzokis, G., Nuechterlein, K. H., Marder, S. R., Mintz, J., Dery, K., & Laack, K. 1996. Age at Illness Onset and Left Temporal Lobe Length in Males with Schizophrenia. *Psychiatry Res.*, **67(3)**, 189–201.

Blackwood, D. H., Young, A. H., McQueen, J. K., Martin, M. J., Roxborough, H. M., Muir, W. J., Clair, D. M. St, & Kean, D. M. 1991. Magnetic Resonance Imaging in Schizophrenia: Altered Brain Morphology Associated With P300 Abnormalities and Eye Tracking Dysfunction. *Biol. Psychiatry*, **30(8)**, 753–769.

Bookstein, F. L. 1997. Landmark Methods for Forms Without Landmarks: Morphometrics of Group Differences in Outline Shape. *Medical Image Analysis*, **1**(3), 225–243.

Cao, J., & Worsely, K. J. 1997. The Geometry of the Hotelling's T^2 Random Field with Applications to the Detection of Shape Changes. *Submitted to Annals of Statistics.*

Cao, J., Worsley, K. J., Liu, C., Collins, L., & Evans, A. C. 1997. New Statistical Results for the Detection of Brain Structural and Functional Change using Random Field Theory. *NeuroImage*, **5(4)**, 512.

Ciesielski, K. T., & Knight, J. E. 1994. Cerebellar Abnormality in Autism: a Nonspecific Effect of Early Brain Damage? *Acta. Neurobiol. Exp. (Warsz)*, **54(2)**, 151–154.

Crow, T. J. 1990. Temporal lobe asymmetries as the key to the etiology of schizophrenia. *Schizophr Bull*, **16(3)**, 433–443.

Frazier, J. A., Giedd, J. N., Kaysen, D., Albus, K., Hamburger, S., Alaghband-Rad, J., & JL, M. C. Lenane McKenna K; Breier A; Rapoport. 1996. Childhood-Onset Schizophrenia: Brain MRI Rescan after 2 Years of Clozapine Maintenance treatment. *Am. J. Psychiatry*, **153(4)**, 564–566.

Friston, K. J., Frith, C. D., Frackowiak, R. S. J., & Turner, R. 1995a. Characterizing Dynamic Brain Responses with fMRI: A multivariate Approach. *NeuroImage*, **2**, 166–172.

Friston, K. J., Ashburner, J., Frith, C. D., Poline, J.-B., Heather, J. D., & Frackowiak, R. S. J. 1995b. Spatial Registration and Normalization of Images. *Human Brain Mapping*, **2**, 165–189.

Gaffney, G. R., Kuperman, S., Tsai, L. Y., & Minchin, S. 1989. Forebrain Structure in Infantile Autism. *J. Am. Acad. Child Adolesc. Psychiatry*, **28(4)**, 534–537.

Geschwind, N., & Galaburda, A. M. 1987. *Cerebral Lateralization, Biological Mechanisms, Associations and Pathology.* Cambridge Mass.: MIT Press. Pages 21–34.

Jacobsen, L. K., Giedd, J. N., Vaituzis, A. C., Hamburger, S. D., Rajapakse, J. C., Frazier, J. A., Kaysen, D., Lenane, M. C., McKenna, K., Gordon, C. T., & Rapoport, J. L. 1996. Temporal Lobe Morphology in Childhood-onset Schizophrenia. *Am. J. Psychiatry*, **153(3)**, 355–361.

Krzanowski, W. J. 1988. *Principles of Multivariate Analysis - A Users Perspective.* Oxford.

Lieberman, J., Bogerts, B., Degreef, G., Ashtari, M, Lantos, G., & Alvir, J. 1992. Qualitative Assessment of Brain Morphology in Acute and Chronic Schizophrenia. *Am. J. Psychiatry*, **149(6)**, 784–794.

Murphy, D. G., DeCarli, C., Daly, E., Haxby, J. V., Allen, G., White, B. J., McIntosh, A. R., Powell, C. M., Horwitz, B., & Rapoport, S. I. 1993. X-Chromosome Effects on Female Brain: a Magnetic Resonance Imaging Study of Turner's Syndrome. *Lancet*, **342(8881)**, 1197–1200.

Nasrallah, H. A., Schwarzkopf, S. B., Olson, S. C., & Coffman, J. A. 1990. Gender Differences in Schizophrenia on MRI Brain Scans. *Schizophr. Bull.*, **16(2)**, 205–210.

Noga, J. T., Aylward, E., Barta, P. E., & Pearlson, G. D. 1995. Cingulate Gyrus in Schizophrenic Patients and Normal Volunteers. *Psychiatry Res.*, **61(4)**, 201–208.

Nopoulos, P., Torres, I., Flaum, M., Andreason, N. C., & Ehrhardt, J. C. 1995. Brain Morphology in First-Episode Schizophrenia. *Am. J. Psychiatry*, **152(12)**, 1721–1723.

Reiss, A. L., Mazzocco, M. M., Greenlaw, R., Freund, L. S., & Ross, J. L. 1995. Neurodevelopmental Effects of X Monosomy: a Volumetric Imaging Study. *Ann. Neurol.*, **38(5)**, 731–738.

Suddath, R. L., Christison, G. W., Torrey, E. F., Casanova, M. F., & Weinberger, D. R. 1990. Anatomical Abnormalities in the Brains of Monozygotic Twins Discordant for Schizophrenia. *N. Engl. J. Med.*, **322(12)**, 789–794.

Tsai, L. Y., Jacoby, C. G., & Stewart, M. A. 1983. Morphological Cerebral Asymmetries in Autistic Children. *Biol. Psychiatry*, **18(3)**, 317–327.

Wright, I. C., McGuire, P. K., Poline, J.-B., Travere, J. M., Murray, R. M., Frith, C. D., Frackowiak, R. S. J., & Friston, K. J. 1995. A Voxel-Based Method for the Statistical Analysis of Gray and White Matter Density Applied to Schizophrenia. *NeuroImage*, **2**, 244–252.

A Multivariate Analysis of Covariance and Canonical Variates Analysis

The analysis may be confounded by a number of possible effects. For the analysis described here, the confounds are modeled by an $m \times g$ design matrix $\mathbf{G}$. Each column of $\mathbf{G}$ can be a vector of covariates, or alternatively can be arranged in blocks for group specific estimation. The mean is removed from the data by including a constant column in $\mathbf{G}$. Any variance in the data ($m \times n$ matrix $\mathbf{A}$) that could be attributed the confounds is removed by:

$$\mathbf{A_a} = \mathbf{A} - \mathbf{G}\left(\mathbf{G}^T\mathbf{G}\right)^{-1}\mathbf{G}^T\mathbf{A}$$

Similarly, the effects of interest are modeled by an $m \times c$ design matrix $\mathbf{C}$. The columns in this design matrix are orthogonalized with respect to matrix $\mathbf{G}$:

$$\mathbf{C_a} = \mathbf{C} - \mathbf{G}\left(\mathbf{G}^T\mathbf{G}\right)^{-1}\mathbf{G}^T\mathbf{C}$$

The ManCova involves assessing how the predictability of the observed deformation parameters change when the effects of interest are discounted. This involves the distributions of the residuals that are assumed to be multinormal. The statistic is related to the determinants of the covariance matrices describing these distributions. In practice, the residual sum of squares and products (SSP) matrix ($\mathbf{W_0}$), is compared to the SSP matrix of the fitted effects ($\mathbf{B_0}$). These matrixes are obtained by:

$$\begin{aligned}\mathbf{T} &= \mathbf{C_a}\left(\left(\mathbf{C_a}^T\mathbf{C_a}\right)^{-1}\mathbf{C_a}^T\mathbf{A_a}\right)\\ \mathbf{B_0} &= \mathbf{T}^T\mathbf{T}\\ \mathbf{W_0} &= (\mathbf{A_a}-\mathbf{T})^T(\mathbf{A_a}-\mathbf{T})\end{aligned}$$

The statistic is called *Wilk's Lambda* (Λ), and is based upon the ratios of the determinants (see Krzanowski (1988) for a more detailed explanation):

$$\Lambda = \frac{|\mathbf{W_0}|}{|\mathbf{B_0}+\mathbf{W_0}|}$$

This statistic is transformed to a χ^2 statistic (with nc degrees of freedom under the null hypothesis) using the approximation of Bartlett:

$$\chi^2 \approx ((n-c+1)/2-(m-c-g))log_e(\Lambda)$$

Finally, the cumulative χ^2 distribution function is used to make inferences about whether the null hypothesis (that there is no difference between the distributions) can be rejected.

Canonical variates analysis (CVA) can be used to characterize any effects of interest. The vectors that best discriminate between the groups are obtained from the c eigenvectors of $\mathbf{B_0}$ (e.g., differences in figure 5) or $\mathbf{W_0}^{-1}\mathbf{B_0}$ (i.e., the canonical vectors ϵ in figure 4) that have non-zero eigenvalues. The corresponding canonical variates are given by $\mathbf{A_a}\epsilon$.

B Partitioning the Deformation Fields into Positional, Size and Shape Components

The deformation fields are defined by both non-linear and affine components. In order to proceed, it is necessary to decompose the transformation into components relating to position and size (uninteresting components), and shape (the components that we are interested in). In order to effect this decomposition, each deformation field was reconstructed from it's parameters. Each field provides a mapping from points in the template to points in the image, allowing standard landmark based registration methods to be used to extract the size and positional information. Rather than basing the registration on a few landmarks, all the elements of the deformation field corresponding to voxels within the brain were considered (by weighting with the image shown in figure 1). This involved first determining the translations by computing centers of mass:

$$\bar{\mathbf{x}} = \frac{\sum_{i=1}^{I} \mathbf{x}_i w_i}{\sum_{i=1}^{I} w_i}$$
$$\bar{\mathbf{y}} = \frac{\sum_{i=1}^{I} \mathbf{y}_i w_i}{\sum_{i=1}^{I} w_i}$$

where $\mathbf{x}_i$ is the co-ordinate of the ith voxel of the template, $\mathbf{y}_i$ is the location that it maps to, and w_i is the weighting for that element. The rotations were computed from the cross-covariance matrix ($\mathbf{C}$) between the elements and deformed elements (after removing the effects of position):

$$c_{j,k} \propto \sum_{i=1}^{I} w_i (x_{i,j} - \bar{x}_j)(y_{i,k} - \bar{y}_k)$$

The 3×3 matrix $\mathbf{C}$ was decomposed using singular value decomposition to give three matrixes, $\mathbf{U}$, $\mathbf{S}$ and $\mathbf{V}$ (such that $\mathbf{C} = \mathbf{USV}^T$, where $\mathbf{U}$ and $\mathbf{V}$ are unitary, and $\mathbf{S}$ is a diagonal matrix). The rotation matrix ($\mathbf{R}$) could then be reconstituted from these matrixes by $\mathbf{R} = \mathbf{UV}^T$. Finally, moments around the centers were used to correct for relative size differences (z):

$$z = \sqrt{\frac{\sum_{j=1}^{3} \sum_{i=1}^{I} (x_{i,j} - \bar{x}_j)^2 w_i}{\sum_{j=1}^{3} \sum_{i=1}^{I} (y_{i,j} - \bar{y}_j)^2 w_i}}$$

After removing the effects of translation, rotation and scaling from the deformation fields, they were then reparameterized by the lowest frequency coefficients of their three dimensional DCTs.

List of Figures

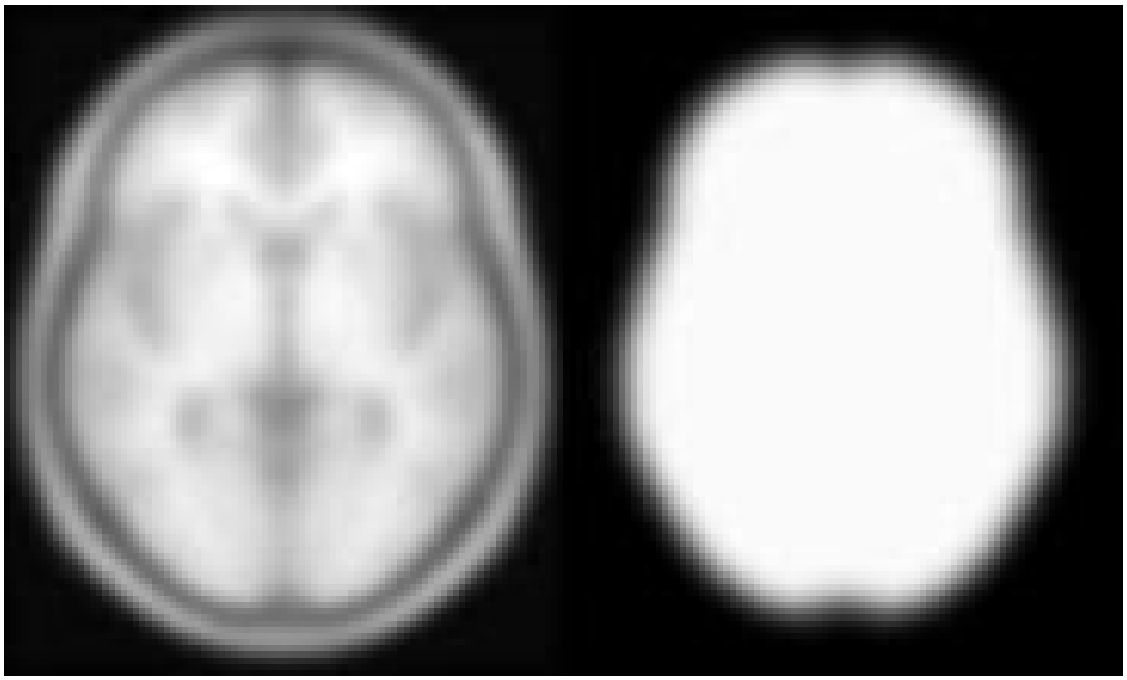

Figure 1: The template (left) and weighting image (right) used by the registration. Note that the images have been smoothed using an 8mm full width at half maximum isotropic Gaussian kernel in order to facilitate the registration.

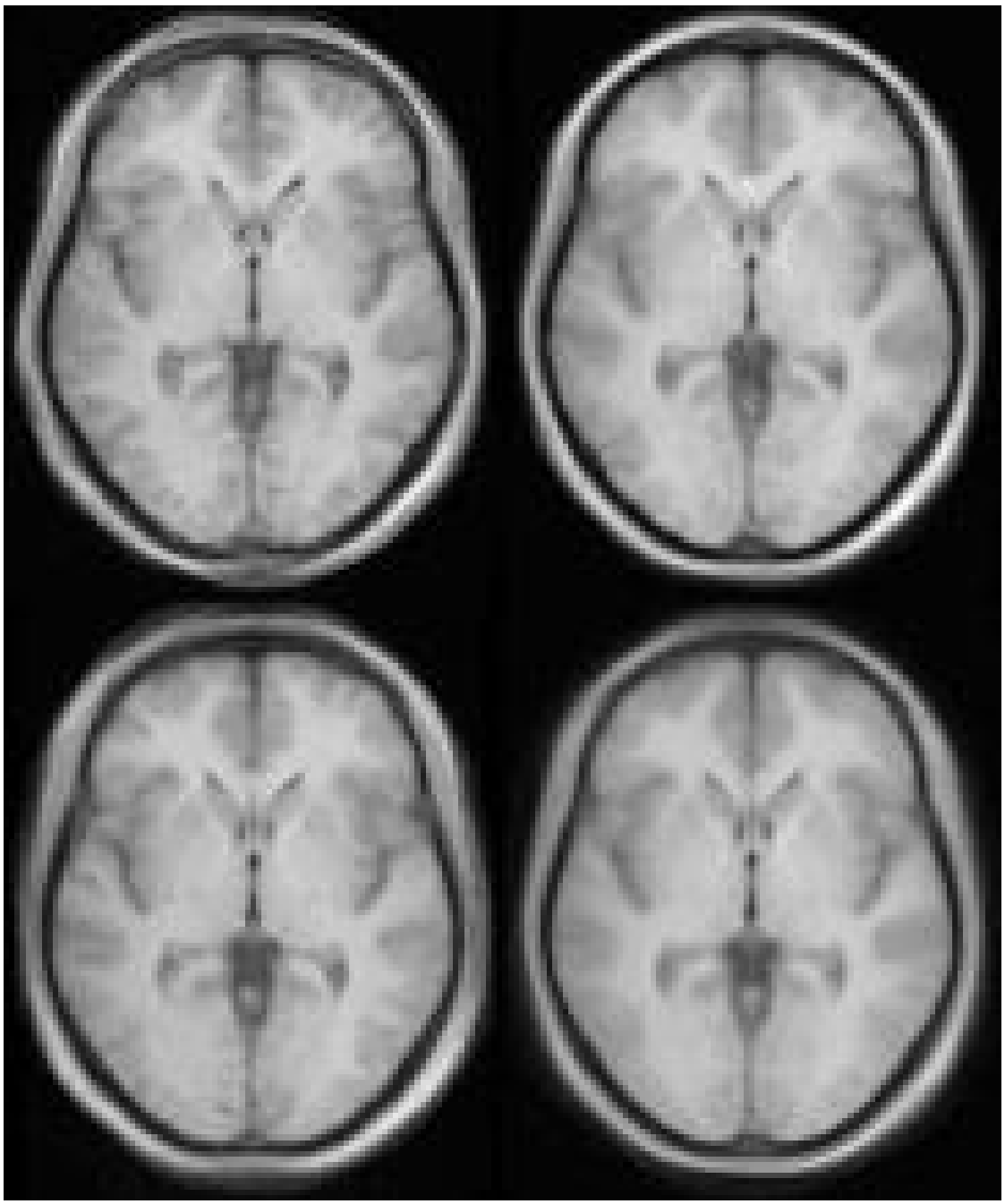

Figure 2: The mean of the spatially normalized images for each group: left handed females (above left), right handed females (above right), left handed males (below left) and right handed males (below right).

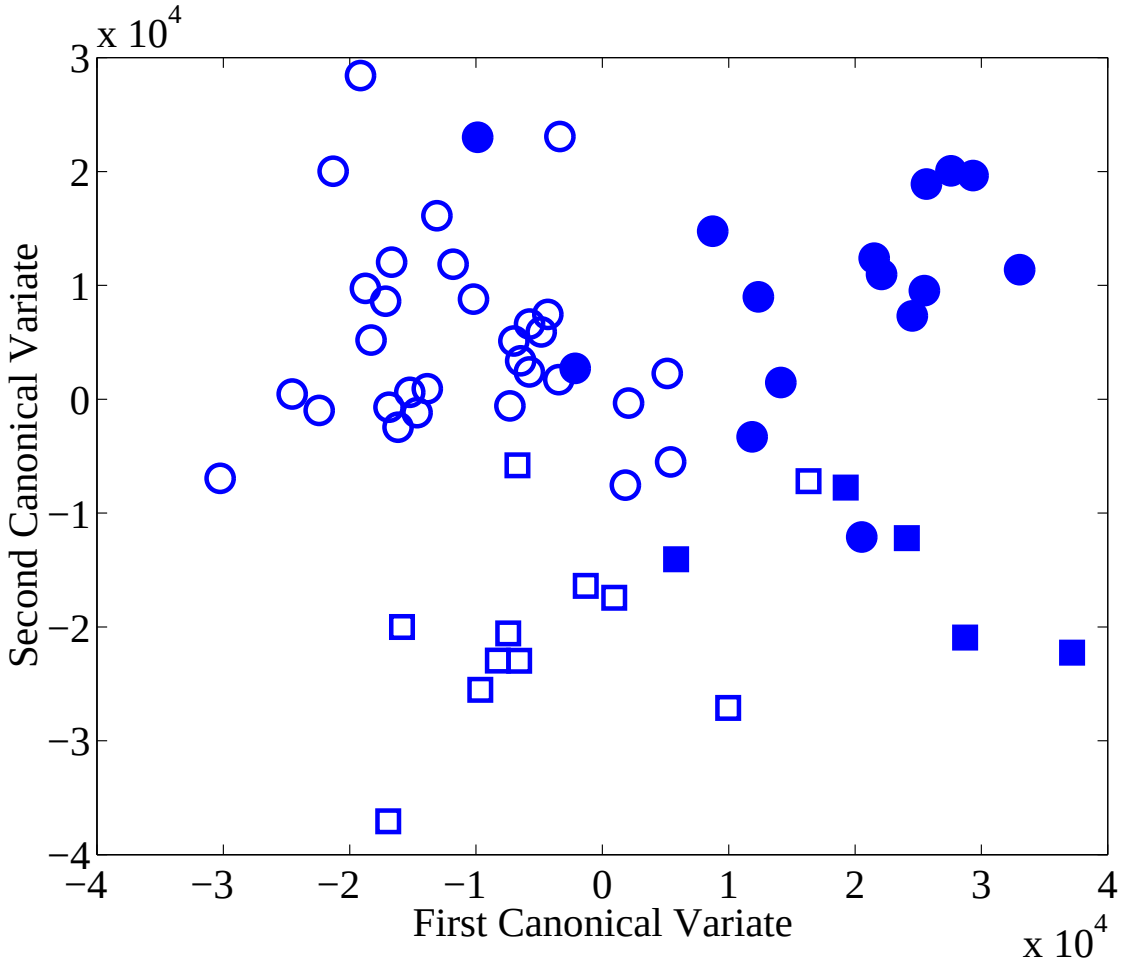

Figure 3: Separation of subjects using canonical variates analysis. Right handed females (filled circles), left handed females (filled squares), right handed males (empty circles) and left handed males (empty squares).

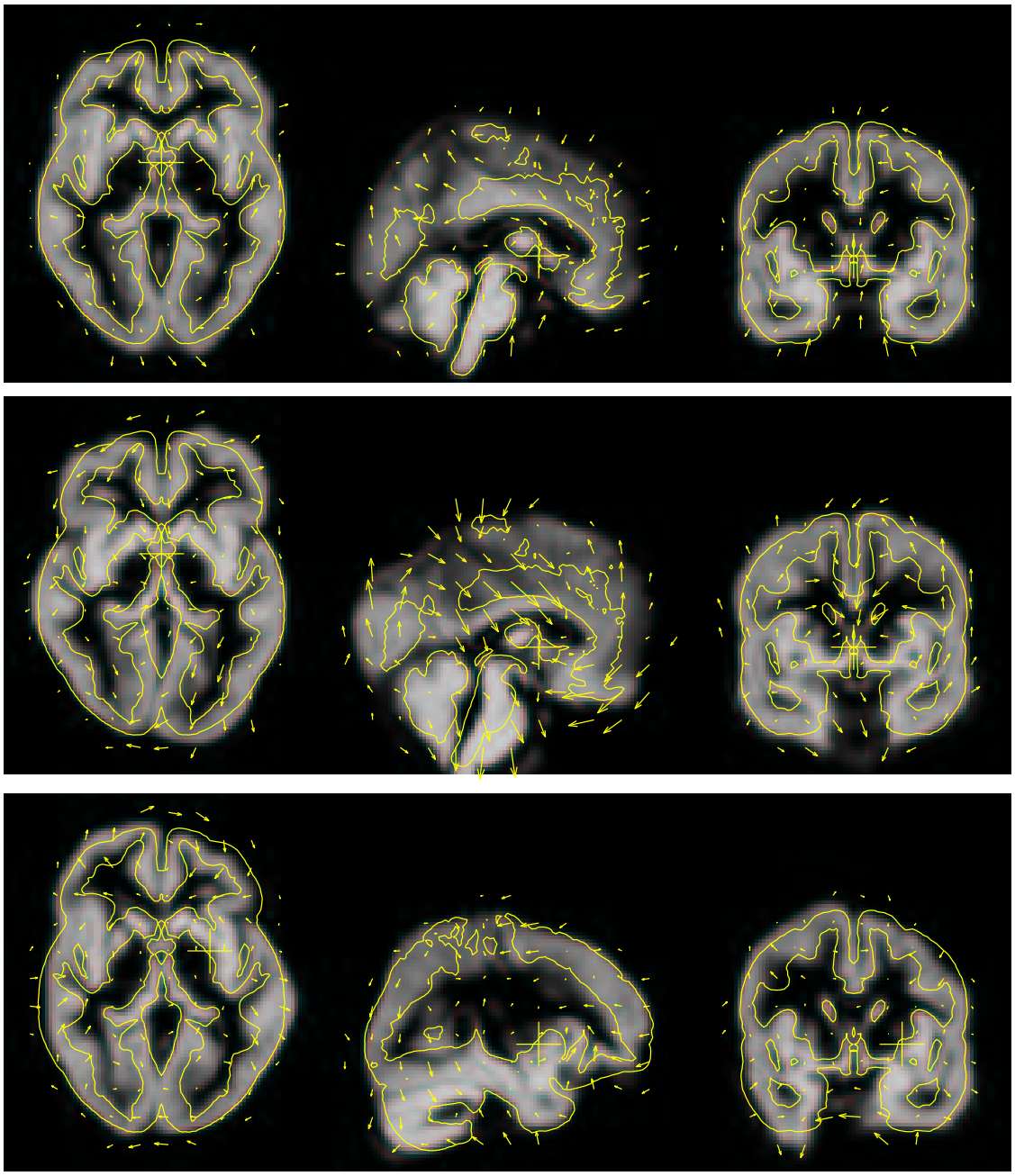

Figure 4: Nonlinear warps pertaining to sex differences (above), handedness differences (center), and asymmetry (below) characterized by canonical variates analysis. The images of gray matter show a caricature of the deformations. Superimposed on this is a contour from the undeformed image. The arrows show the direction of the nonlinear warps characterized by CVA. These are not the mean differences between the brain shapes, but rather the differences that most clearly distinguish them. In the transverse and coronal sections, the left side of the brain is on the left side of the figure.

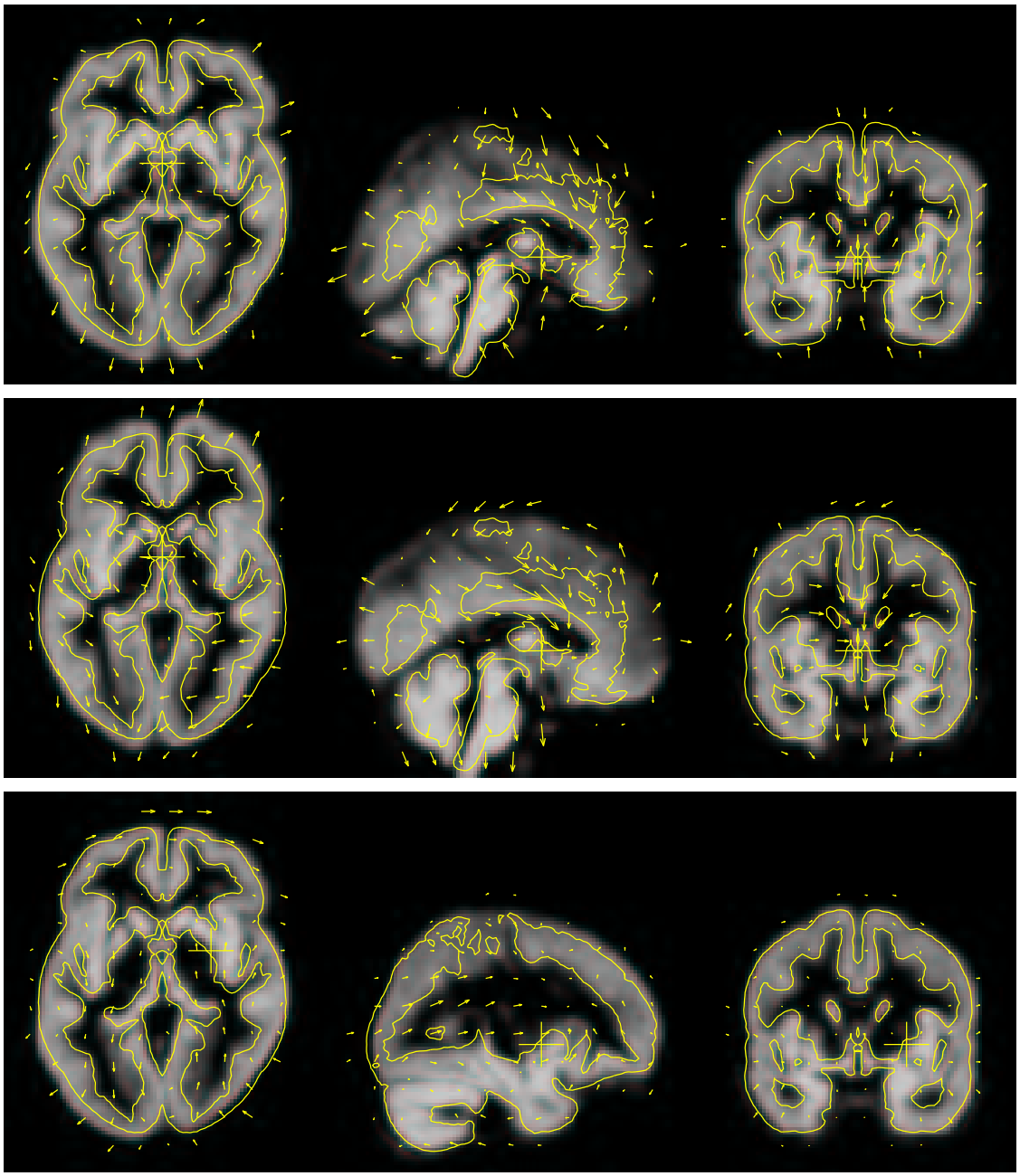

Figure 5: The deformation required to map from a female to male brain (above), left-handed to right-handed brain (center), and antisymmetric deformations from a symmetric template to an asymmetric brain (below), all multiplied by a factor of 5. The deformations were computed after first removing the effects of confounds, and are a direct characterization of the parameter estimates without referring to the errors or reliability of the differences (c.f., CVA).